Journal of the Serbian Society for Computational Mechanics / Vol. 17 / No. 2, 2023 / pp 125-141
(10.24874/jsscm.2023.17.02.09)

MAGNETOHYDRODYNAMICS AND POWER-LAW FLUIDS IN DOUBLE LID-DRIVEN CAVITY WITH SEMI-CIRCULAR BODIES

Abdeljalil Benmansour* **and Hacène Hamoudi**

Faculty of Mechanical Engineering, University of Science and Technology of Oran, Mohammed Boudiaf, B.O. Box 1505, El-M'Naouer, 31000, Oran, Algeria
e-mail: benmansour.abdeljalil@yahoo.fr

**corresponding author*

Abstract

The use of complex fluids is one of the modern techniques used in small devices in order to enhance their thermal performance. This paper is a numerical study of a complex fluid imprisoned in a chamber with two hot bodies exposed to a magnetic field of constant intensity. The upper and lower walls move horizontally at a constant velocity, while the lateral sides are thermally insulated. The numerical simulation of the system was achieved based on the finite volume method that solves the differential equations of fluid mechanics and heat transfer. Simulations were carried out under the following conditions: Re = 1 to 40, Ri = 0 to 100, n = 0.6 to 1.4 and Ha = 0 to 100. The study showed that the thermal activity of the two bodies is different and related to initial condition. Also, the effect of the magnetic field is strong in the case of shear-thinning fluids, while its effect is diminished in the case of shear-thickening fluids.

Keywords: Ostwald model, Lorentz force, thermal buoyancy, heat transfer, steady simulation.

1. Introduction

Thermal transfer is one of the necessary studies in all fields of life due to its importance in engineering application and technology. On other hand, thermal systems are witnessing a rapid development, which is mainly reflected in reducing the size of the system and strengthening its thermal activity. We can notice the presence of thermal systems in all fields, such as small thermal exchangers, solar panels and cooling systems used in electronics.

Studies have shown that the heat transfer of fluids is related to a set of criteria mainly connected to the geometric shape of the system and the fluid quality (Maneengam et al. 2022; Laidoudi and Bouzit 2018; Aliouane et al. 2021; Selimefendigil 2019; Alsabery et al. 2020; Gangawane et al. 2018). Geometry has an effect on the fluid motion allowing for an effect on heat transfer (Laidoudi and Bouzit 2017; Herouz et al. 2022; Anouar and Mokhefi 2022; Laidoudi, 2020). However, the quality of the fluid affects the thermal properties, which affects the heat capacity and thermal conductivity of the fluid (Abderrahmane et al. 2023; Laidoudi and Ameur 2020; Mohebbi and Rashidi 2017; Usman et al. 2019; Laidoudi and Ameur 2022).

Recently, there has been a lot of research on lid-driven chambers (Laidoudi et al. 2022; Nasrin et al. 2014; Hansda and Pandit 2023; Rais et al. 2023; Chowdhury et al. 2023), due to their

frequent presence in industrial and engineering applications. This type of system is characterized by the horizontal movable wall and the fluid quality with high thermal properties (Rashidi et al. 2021; Yeasmin et al. 2022; Sivanandam and Marimuthu 2023; Hussain and Öztop 2021; Islam et al. 2012; Shuvo et al. 2022). Previous studies on this topic focused on the general shape of the chamber (Peng et al. 2003; Albensoeder and Kuhlmann 2005; Nemati et al. 2010; Esfe et al. 2019), the shape of the hot objects placed inside the chamber (Khanafer and Aithal 2017; Khanafer and Aithal 2013; Kareem and Gao 2017), fluid quality (Hatič et al. 2021; Chowdhury and Kumar 2023; Kefayati 2015) and the effects of internal and external forces (Oztop et al. 2011; Hussain et al. 2016; Chatterjee 2013).

Most of the studies on this topic were performed through numerical simulations, which are mainly based on solving differential equations of fluid mechanics and heat transfer. On other hand, the physical parameters are studied in a non-dimensional quantity. For example, the value of flow movement is expressed by the non-dimensional number of Reynolds; thermal properties are expressed by Prandtl number, etc.

Iftikhar et al. (2023) studied a complex fluid inside a square shaped chamber subjected to magnetic field and thermal buoyancy. The container does not contain any body and has only one movable wall. The study was conducted in a non-dimensional way, as the initial conditions were written in terms of the numbers of Prandtl, Reynolds, Richardson, Grashof and Hartmann. Kardgar (2021) conducted a study on the behavior of a complex fluid inside a square-shaped chamber subjected to magnetic field. The complex fluid is of the power-law. The initial conditions of the simulation were made by non-dimensional numbers of Hartmann, Reynolds, Womersley, power-law index and nanofluid concentration. The study showed that the magnetic field has negative effects on the movement of the flow, as well as the thermal activity. There was a decrease in the values of Nusselt number as the intensity of the magnetic field increased. Javed et al. (2023) also presented a study on a complex fluid inside an I-shaped chamber to which a magnetic field of constant intensity is applied. The parameters studied in this research were: Bi-viscosity, Grashof number, Hartmann and Reynolds numbers, and a decrease of 25.92% of Nusselt number was detected when the magnetic field was utilized.

According to the literature review, it appears that heat transfer inside a lid-driven container is of great importance in many applications; also, despite the existence of a large group of studies on this subject, there are still other cases that have not been studied. For example, the double lid-driven chambers with the presence of heated bodies inside it and under the influence of the magnetic field and the force of thermal buoyancy. For this purpose, this research aims to include new findings about this deficiency. So, our study shows the dynamic behavior of a complex fluid in a double lid-driven chamber containing two semi-circular bodies and an external magnetic field applied to them. The thermal transfer mode used here is of the mixed convection type. Furthermore, the results of this paper can be used in the development of thermal exchangers with small dimensions. This paper can also be referred to in writing educational literature with the aim of providing physical explanations.

2. Studied domain and mathematical formulation

Fig. 1 depicts a simplified illustration of the studied geometry. The geometry consists of two, hot, semi-circular obstacles in a double lid-driven cavity. The lateral walls of the chamber are cold. As for the lower and top walls, they are adiabatic and have a horizontal movement from left to right. The internal space of the geometry is completely filled with power-law liquids known mainly by the index (n) and consistency (m). Besides, an external magnetic field (B0) is applied from left to right. The dimensions of the present geometry are: L = 10 (cm) and d/L = 0.5, and

the space between the semi-circulars is e/L = 0.1 The thermal properties (heat capacity and thermal conductivity) of the working liquid are defined by Prandtl number (Pr = 50).

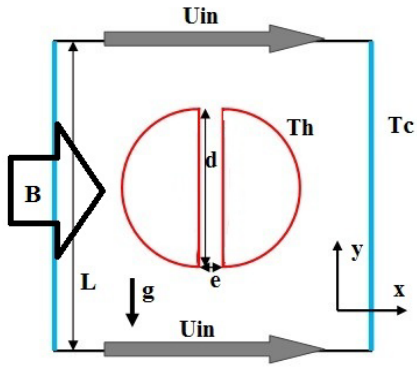

Fig. 1. Studied domain.

Some considerations were taken into account in order to achieve the simulations: the relationship between the temperature and fluid density was treated by the Boussinesq approximation; the dynamic viscosity of the complex fluid was defined by the Oswald model; Joule heating and displacement currents were neglected. The principal equations of fluid mechanics and heat transfer in Cartesian coordinate system are:

$$\frac{\partial u}{\partial x}+\frac{\partial v}{\partial y}=0 \tag{1}$$

$$u\left(\frac{\partial u}{\partial x}\right)+v\left(\frac{\partial u}{\partial y}\right)=-\frac{1}{\rho}\frac{\partial p}{\partial x}+\frac{1}{\rho}\left(\frac{\partial \tau_{xx}}{\partial x}+\frac{\partial \tau_{xy}}{\partial y}\right)+\frac{\sigma B_0^2}{\rho}\left(v\sin(\gamma)\cos(\gamma)-u\sin^2(\gamma)\right) \tag{2}$$

$$u\left(\frac{\partial v}{\partial x}\right)+v\left(\frac{\partial v}{\partial y}\right)=-\frac{1}{\rho}\frac{\partial p}{\partial y}+\frac{1}{\rho}\left(\frac{\partial \tau_{xy}}{\partial x}+\frac{\partial \tau_{yy}}{\partial y}\right)+\frac{\sigma B_0^2}{\rho}\left(u\sin(\gamma)\cos(\gamma)-v\sin^2(\gamma)\right)+\beta g(T-T_c) \tag{3}$$

$$u\left(\frac{\partial T}{\partial x}\right)+v\left(\frac{\partial T}{\partial y}\right)=\alpha\left(\frac{\partial^2 T}{\partial x^2}+\frac{\partial^2 T}{\partial y^2}\right) \tag{4}$$

The dynamic viscosity of the power-law fluids can be defined as:

$$\tau_{ij}=m\left(2\left[\left(\frac{\partial u}{\partial x}\right)^2+\left(\frac{\partial v}{\partial y}\right)^2\right]+\left(\frac{\partial u}{\partial x}+\frac{\partial v}{\partial y}\right)^2\right)^{(n-1)/2}\left(\frac{\partial u_i}{\partial x_j}+\frac{\partial u_j}{\partial x_i}\right) \tag{5}$$

Where m, n indicate consistency and power-law index, respectively. According to the value of the power-law index, we distinguish three cases. When n > 1 means that the fluid is of shear-thickening, the dynamic viscosity of the liquid augments as the friction factor of the flow augments. When n < 1 means that the fluid is of shear- thinning, the dynamic viscosity of the liquid decreases as the frictional factor augments. When n = 1 means that the fluid purely Newtonian, the dynamic viscosity does not depend on the frictional coefficient.

The dimensionless numbers that control the initial conditions are defined as:

$$Pr=\frac{mC_p}{k(u_{in}/L)^{n-1}},\ Re=\frac{\rho(u_{in})^{2-n}L^n}{m},\ Gr=g\beta_T\Delta TD^3\left[\frac{\rho}{m}(u_{in}/L)^{1-n}\right]^2,\ Ri=\frac{Gr}{Re^2}=\frac{g\beta_T\Delta TL^3}{(u_{in})^2},\ Ha=LB_0\sqrt{\frac{\sigma}{\mu}} \tag{6}$$

The exact expression of the dynamic viscosity according the Ostwald model can be given as:

$$\mu=m\left(\frac{I_2}{2}\right)^{\left(\frac{n-1}{2}\right)} \tag{7}$$

The initial boundary conditions for the extremities of the geometry are given:

- On the heated walls of semi-circular obstacles: u = v = 0 and T = T_h.
- On cold side of the container: $u=v=0, T=T_c$
- On the top and bottom walls: $u=v=u_{in}, \frac{\partial T}{\partial ns}=0$

The Nusselt number gives the quantitative value of the heat transfer and it can be calculated as:

$$Nu_L=\left(\frac{\partial T}{\partial ns}\right)_{wall} \text{ and } Nu=\frac{1}{A}\int_s Nu_L dA \tag{8}$$

3. Steps of simulation and validation test

The study of the system is done using ANSYS-CFX. This simulator converts the principal equations of fluid mechanics and heat transfer into a system of matrix. After that, the boundary conditions are exerted on the extremities; solutions are calculated using the numeral method called the finite volume. The value 10^{-6} was adopted as error of calculations for the fluid mechanics and thermal transfer equations. However, high resolution schema was adopted for calculating the convective terms. On other hand, pressure-velocity coupling was adopted by SIMPLEC algorithm. The latter is considered as a method of solving the Navier-stokes equations. It is based on a set of stages to reach the final solution to velocity and pressure components.

Generally, the number of grid elements is one of the criteria that affects the accuracy of calculation, so the number of the grid elements must be determined accurately. For this purpose, we made a study where the number of grid elements was obtained. Table 1 summarizes this process. We produced three types of grids of different densities, and each time we calculated the Nusselt number of the two semi-circular obstacles for the following conditions: Ha = 50, n = 0.8, Re = 40 and Ri = 50. Clearly, GB is very suitable grid for this research, because there is no significant difference in the values of Nusselt compared with GC.

Grid	Elements	Nu(C1)	Nu(C1)
GA	160,000	13.7107	14.2287
GB	320,000	13.7503	14.2541
GC	640,000	13.7511	14.2544

Table 1. Grid independency test for Ha = 50, Re = 40, Ri = 50 and n = 0.8.

We also conducted a study to prove the accuracy of the method used in solving the studied equations. For this purpose, we repeated the same study that Aboueian-Jahromi et al. (2011) had done with the same initial conditions Ha = 0, Re = 20 and Ri = 0. The results of this study are presented in Fig. 2 with the same findings of Aboueian-Jahromi et al. (2011). We note here a

similarity in the results. And therefore, we confirm the accuracy of this method in solving the studied equations. The results of the second validation test are presented in Table 2. The study is about the variation of Nusselt number versus Hartmann number for n =1.4 and Ra = 10^5. In Table 2, the variations of Nu number of heated surface are presented for different values of Ha at n = 1.4 and Ra = 10^5. The comparison was done with the results of Kefayati (2016). Indeed, the results show a good agreement.

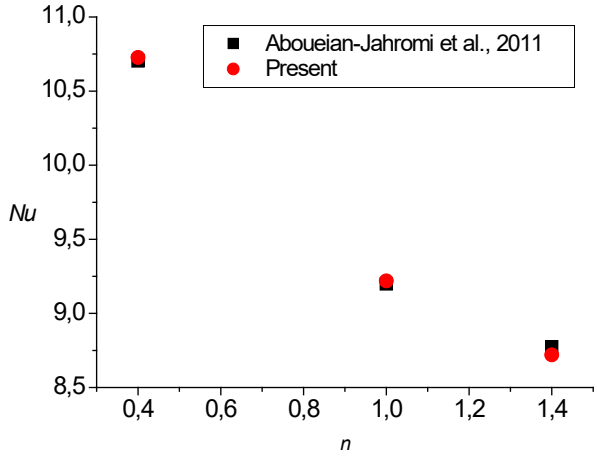

Fig. 2. Validation code for Ha = 25 and 100 at Ra = 7.10^5.

Ha	Nu (Present)	Nu (Kefayati, 2016)	Error%
0	7.6253	7.6222	0.04
15	7.2455	7.2454	0.0013
30	5.6323	5.6313	0.018

Table 2. Validation test, variation of Nu in terms of Ha for n = 1.4 and Ra = 10^5

4. Results and discussion

This study aims to evaluate a comprehensive understanding about the behavior of non-Newtonian fluid inside a chamber with two movable walls (the upper and the lower) and under the influence of both magnetic field as an external factor and the thermal buoyancy as an internal effect. In fact, the research is based on determining the quality of heat transfer between the cold walls of the chamber (lateral walls) and the hot bodies under the influence of the mentioned conditions and under the non-Newtonian behavior of the fluid.

Before we start presenting and analyzing the results, it is worth mentioning some physics concepts that help explain the observations. First, complex or non-Newtonian fluids have a variable viscosity characteristic. That is, the viscosity is related to the velocity of the flow and how closer or far it is from the wall. Secondly, thermal buoyancy is a physical phenomena present in a liquid and gas and it determines the relationship between the density of the fluid and its temperature. That is, the higher the temperature of the fluid, the lighter the fluid becomes, and this is what causes it to move upward. This movement is associated with a quality of thermal energy. That is, it is a movement of matter with energy. Finally, we mention the magnetic field

and its effect on liquids. The presence of the magnetic field incites the presence of a force inside the fluid called the Lorentz force, which affects the movement of the flow.

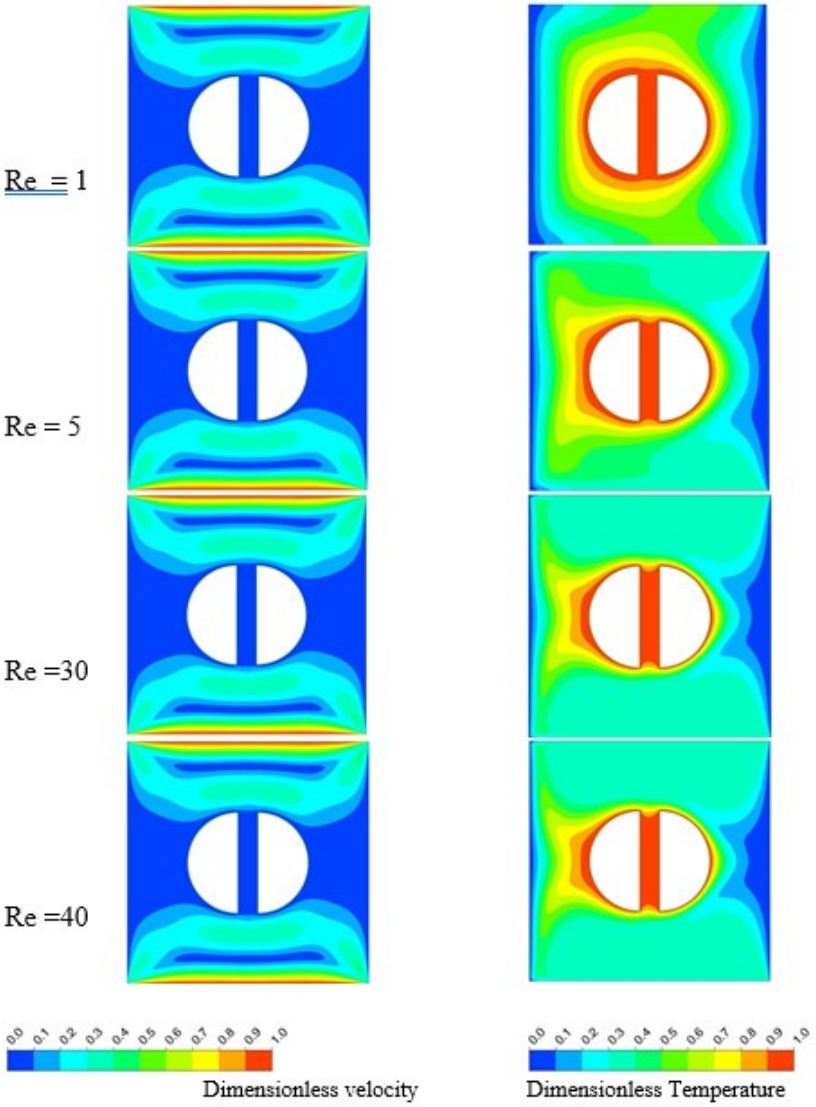

Fig. 3. Contours of dimensionless velocity and temperature in terms of Reynolds number for n = 1, Ri = 0 and Ha = 0.

Fig. 3 presents evolutions of the dimensionless velocity and dimensionless temperature contours in terms of Reynolds number for n = 1, Ri = 0 and Ha = 0. The Reynolds number determines the speed of the movement of the upper and lower walls. The higher the Re value, the faster the wall. n = 1, means that the fluid is Newtonian. Ri = 0 means that there is no effect of thermal buoyancy, also Ha = 0 means that there is no strength of magnetic field. It is noted that there is a symmetry in all contours of velocity and temperature. The value of the dimensionless velocity is higher near the upper and lower walls as they are the main source of the fluid

movement. It is concluded that there is a circular motion of the fluid in the upper and lower parts of the container, which forms a constant vortex at the top and bottom parts. Because the movement of the walls is from the left to right, it is noticed that the layers of cold fluid spread on the right side, and the expansion of these layers increases gradually with the increase in the speed of the walls. The latter behavior indicates that the body on the right side (C1) is subjected to higher thermal activity compared to the other body (C2).

Fig. 4 presents the evolutions of Nusselt number (Nu) of hot bodies (C1 and C2) in terms of Re number for n = 1, Ha = 0 and Ri = 0. We point out that the higher the value of Nu, the higher the heat transfer of the heated body. Here we notice an increase in the values of Nusselt number in terms of Re number. It is also noted that the values of the body on the right (C1) are higher than the values of the other body (C2), because the first one (C1) is exposed to a cold flow compared to the second.

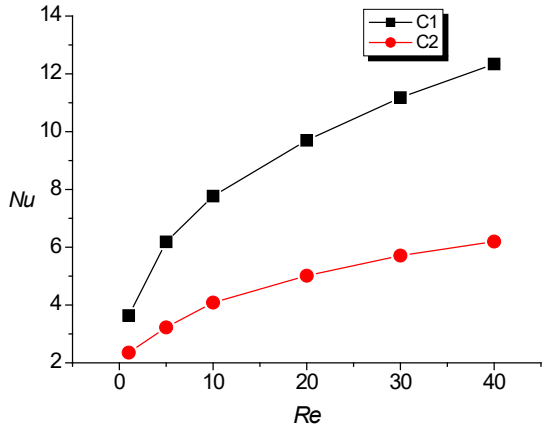

Fig. 4. Variation of Nusselt number of C1 and C2 bodies in terms of Re for n = 1, Ha = 0 and Ri = 0.

Fig. 5 shows the evolution of the flow velocity and temperature in terms of Ri for n = 1, Ha = 0 and Re = 40. Increasing the value of Ri indicates the wide difference in temperature between the hot bodies and cold walls, and this is what makes the thermal buoyancy force higher. Fig. 5 shows that the higher the value of Ri, the greater the dimensionless velocity and temperature inside the chamber, and an asymmetric distribution of velocity and temperature appears. It is noted that the degree of asymmetry increases gradually with augmenting the Ri number. For the flow, a wider spread of the flow velocity is observed, especially near the cold walls and the two hot bodies. As for the temperature contours, we notice that the hot spots are directed upwards, while the cold spots are directed downwards. As we mentioned earlier, increasing the thermal buoyancy force causes the hot fluid spots to move upwards, and this is confirmed by Fig. 5. Through our observation of Fig. 5, we deduce that the thermal activity of the two bodies increases as a result of the increase in thermal buoyancy force.

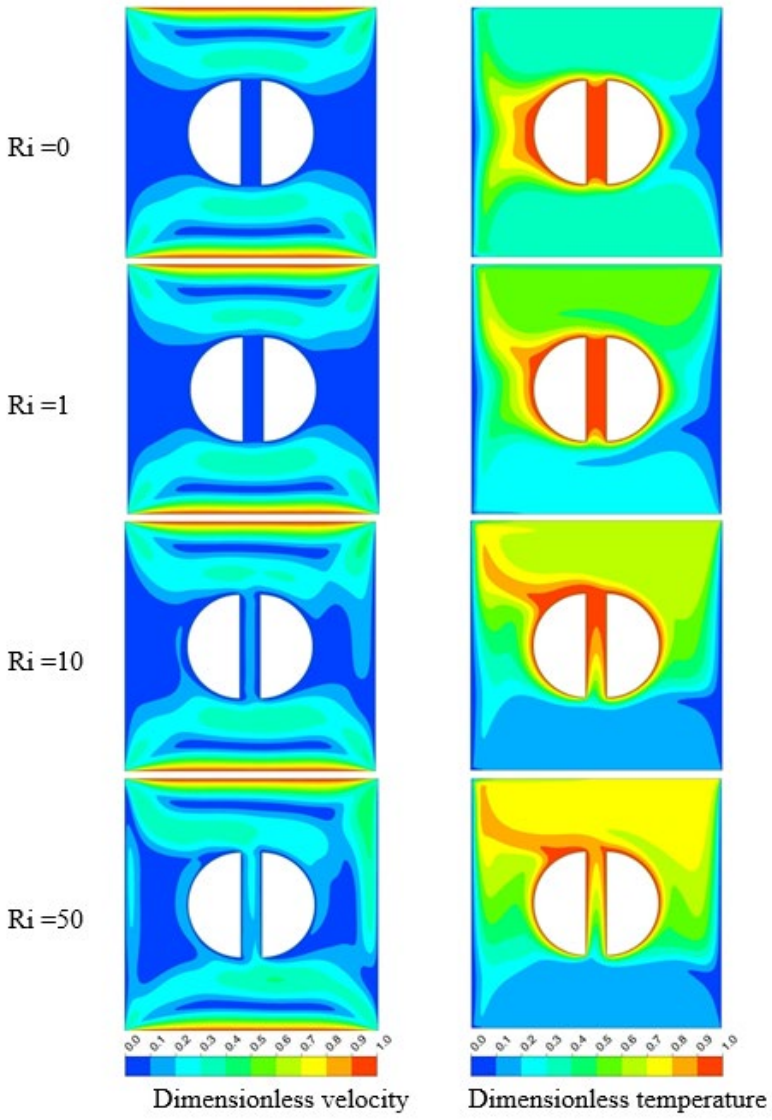

Fig. 5. Contours of dimensionless velocity and temperature in terms of Richardson number for n = 1, Re = 40 and Ha = 0.

Fig. 6 shows the variation of Nusselt of the two bodies C1 and C2 in terms of Ri for Re = 40, Ha = 0 and n = 1. We notice initially that the values of Nusselt number evolve significantly in terms of Ra. Note also that below the value 10 of Ra, the values of Nu of C1 are greater than C2, whereas, above the value 10 of Ra, the values of Nu of C2 becomes greater than of C1. However, Nu values for the two bodies become equal when Ra = 10. It is concluded from Fig. 6 that the presence of thermal buoyancy in the studied system strengthens the heat transfer of the two bodies, especially the body C2.

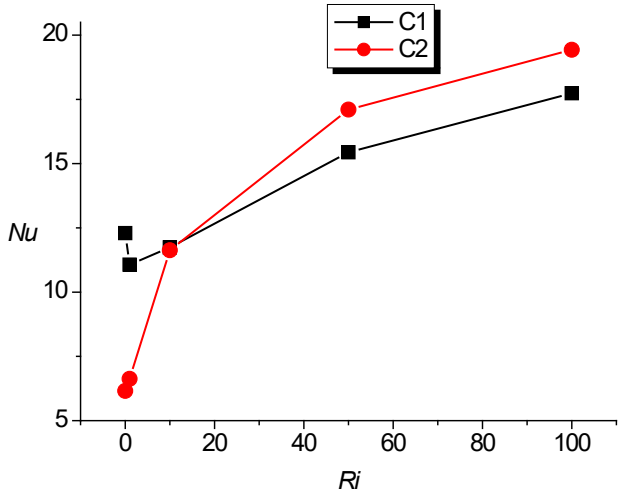

Fig. 6. Variation of Nusselt number of C1 and C2 bodies in terms of Re for n = 1, Ha = 0 and Ri = 0.

Fig. 7 shows the contours of the distribution of dimensionless velocity and dimensionless temperature inside the chamber in terms of the power-law index (n) for Ha = 0, Ri = 50 and Re = 40. The index n determines the rheological nature of the fluid, so when the value of n is less than 1, this indicates that the viscosity decreases as the friction coefficient of the fluid layers increases, while the viscosity increases in terms of the friction coefficient when n values are higher than 1. On other hand, the viscosity is constant when $n = 1$. Through Fig. 7 it appears that the spread of the velocity inside the chamber gradually decreases as the power-law index increases, because the dynamic viscosity of the fluid becomes stronger, which makes the movement of the fluid more difficult. On other hand, we note that the index n slows down the effectiveness of thermal buoyancy, and we notice a slowdown in the spread of temperature. Based on the thermal distribution, it can be concluded that the index *n* negatively affects the thermal transfer of the two hot bodies. In addition to this, we notice that the movement of the flow around the two bodies, as well as the temperature distribution, differs between the body on the right and the body on the left. This is, of course, due to the direction of movement of the upper and lower walls, as well as the amount of dynamic viscosity, which depends on the index n. Also, the upward thermal diffusion of the fluid gradually decreases as the factor n increases, because the fluid becomes more cohesive, making the thermal buoyancy effect less.

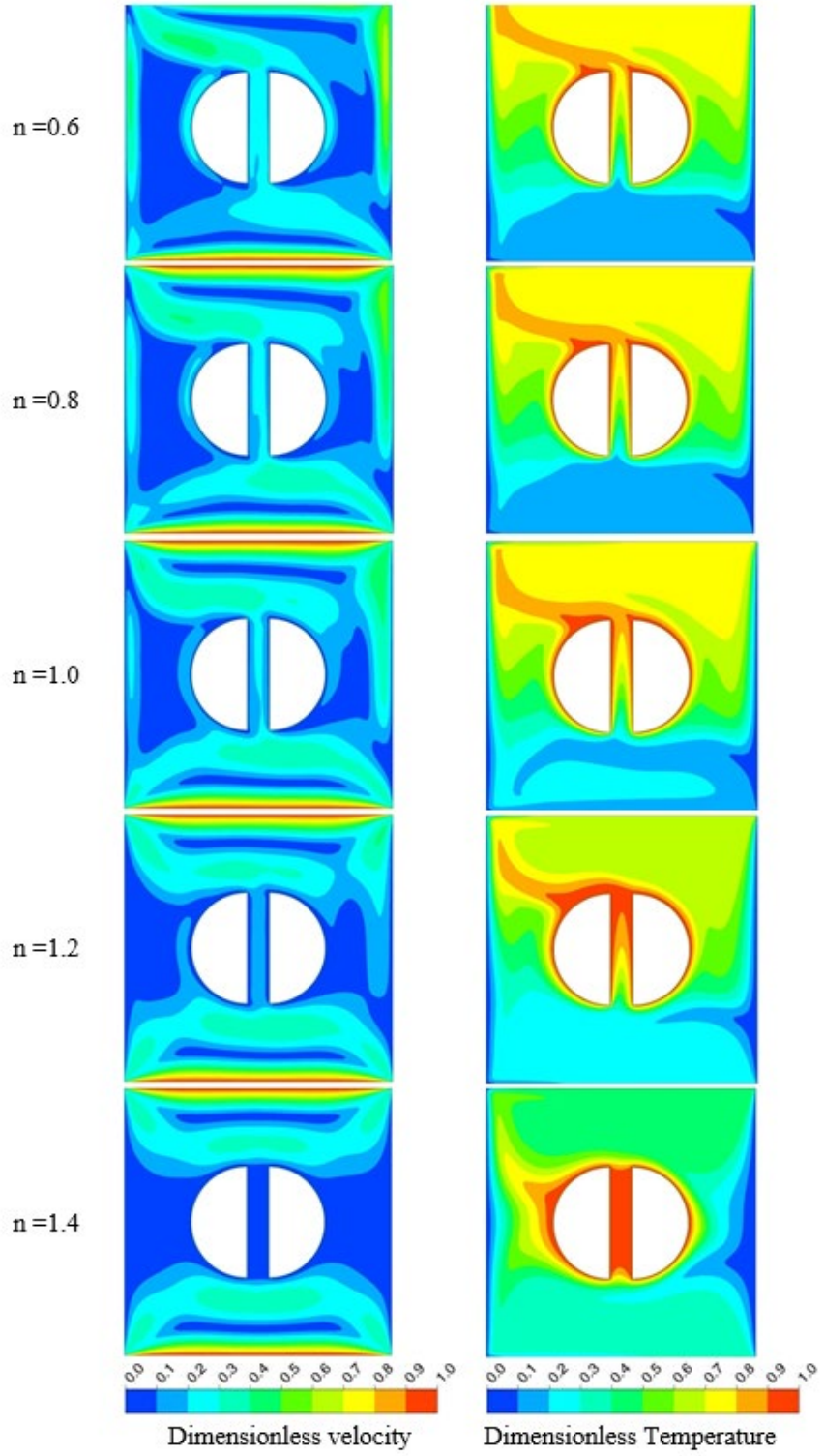

Fig. 7. Contours of dimensionless velocity and temperature in terms of power-law index for Ri = 50, Re = 40 and Ha = 0.

Fig. 8 represents the evolution of the values of Nusselt number of the two bodies in terms of the index *n* for Re = 40, Ha = 0 and Ri = 50. As previously expected, the gradual increase of the index *n* negatively affected the Nusselt number of bodies C1 and C2. It is also noted that when n is less than 1.2, the values of the body C2 are higher than C1. While the values of C1 become the highest when n exceeds 1.2. the Nu values are equivalent to n = 1.2.

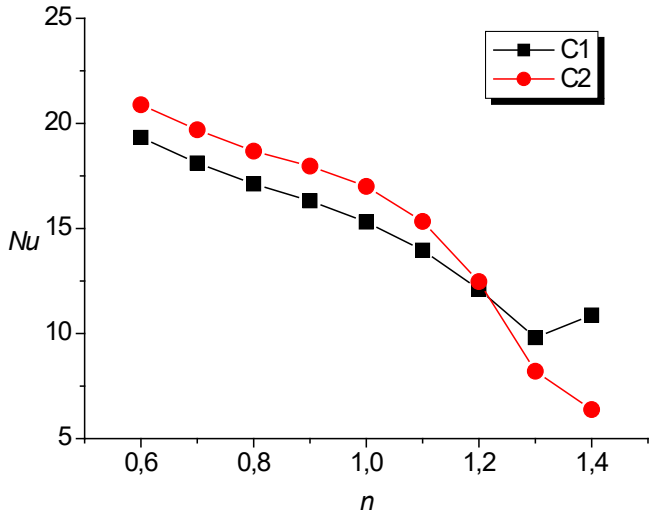

Fig. 8. Variation of Nusselt number of C1 and C2 bodies in terms of N for Re = 40, Ha = 0 and Ri = 50.

Fig. 9 presents contours of the dimensionless velocity in the chamber in terms of the gradual increase of Hartmann number and power-law index (Ha = 0 to 100 and n = 0.8 to 1.4) for Re = 40 and Ri = 50. For the three values of power-law index, increasing the value of Ha reduces the velocity of the flow in the chamber, especially near the side walls of the chamber and near the two hot bodies. It is also noted that this decrease is related to the gradual increase in the value of Ha. Naturally, this decrease in dimensionless velocity is due to the Lorentz force. The effect of this force is opposite to the movement of the flow. On other hand, we notice that the effect of Ha values on the dimensionless velocity decreases gradually as the power-law index increases. It means that the effect of the magnetic field is very strong on the shear-thinning fluids, while this effect decreases for shear-thickening fluids. We note here that the presence of magnetic activity impedes the movement of the flow as a result of the creation of the Lorentz force, which impedes the movement of the flow. On other hand, it is noted that the effect of this force decreases as the index n increases. We conclude here that shear-thickening fluids have high resistance to the magnetic field compared to shear-thinning and Newtonian fluids.

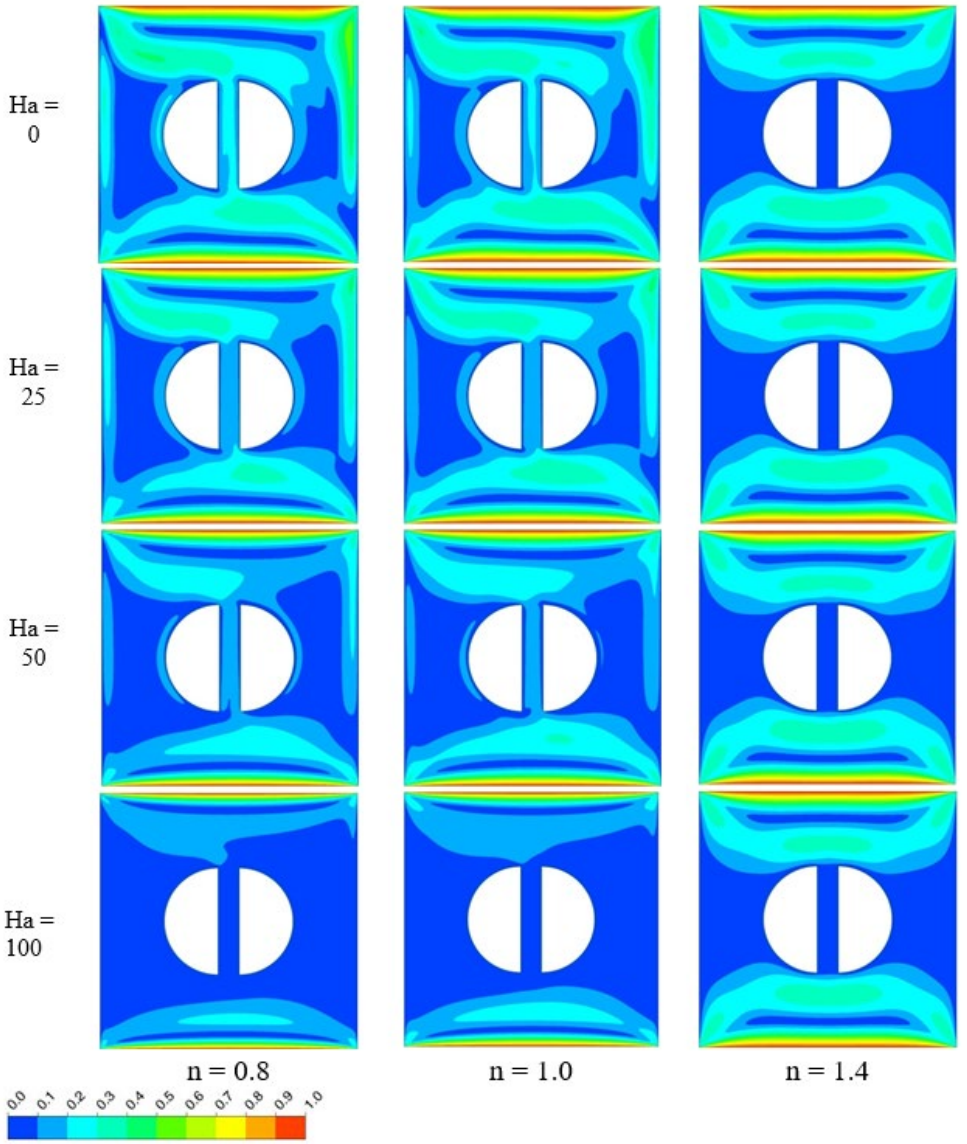

Fig. 9. Contours of dimensionless velocity in terms of Hartmann number and power-law index for Ri = 50 and Re = 40.

Fig. 10 shows the contours of dimensionless temperature in terms of Hartmann number and power-law index for Re = 40 and Ri = 50. We notice that the effect of temperature distribution is quite similar to the contours of dimensionless velocity. So, whenever the value of Ha or n increase, we notice a decrease in the distribution of cold spots of fluid, and this is of course due to a decrease in the velocity of the flow in the container. Furthermore, the effect of Hartmann number on dimensionless temperature decreases as the power-law index n increases, because the viscosity of the fluid becomes more effective. It is concluded here that the heat transfer of two bodies decreases as the value of Ha increases. Also, the effect of Ha on the thermal transfer of hot bodies decreases as the index n increases.

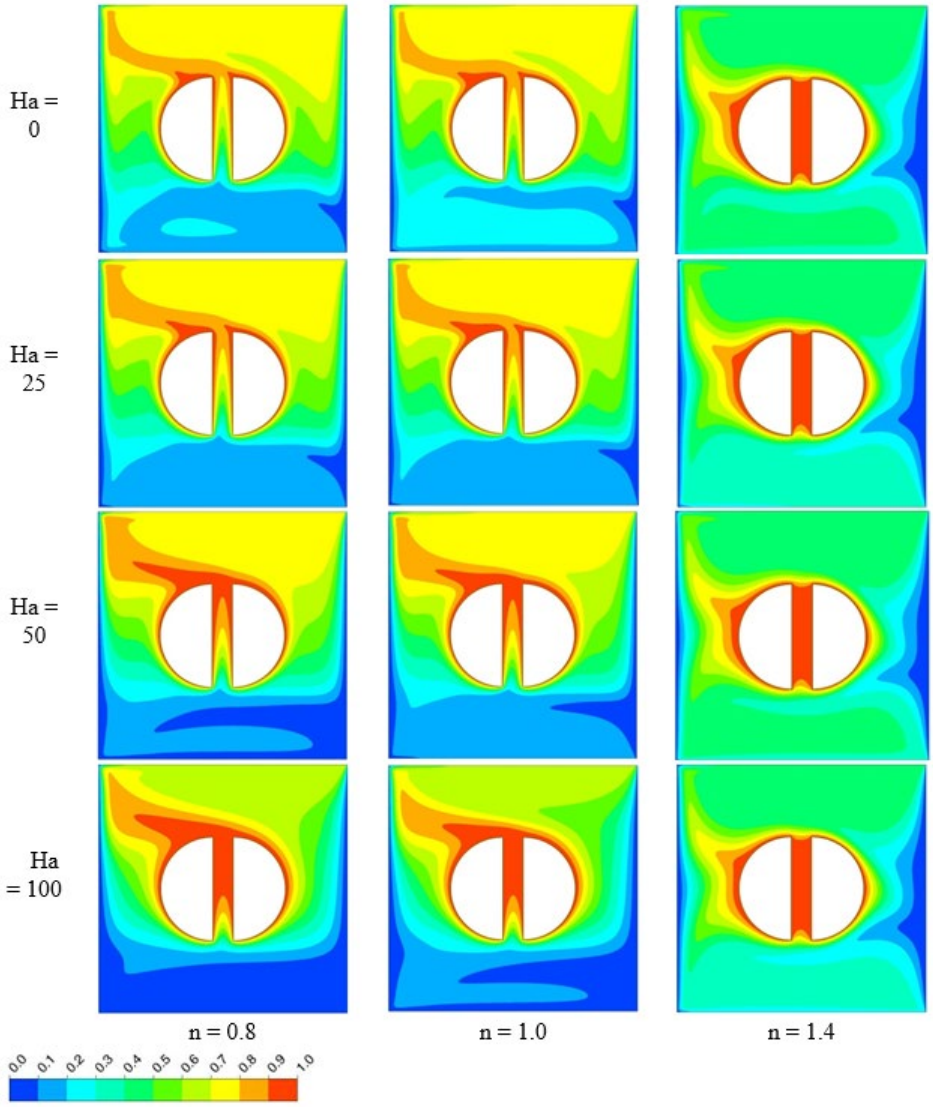

Fig. 10. Contours of dimensionless temperature in terms of Hartmann number and power-law index for Ri = 50 and Re = 40.

Fig. 11 shows the variation of average Nusselt number of the two hot bodies (C1 and C2) in terms of Hartmann number and power-law index (n) for Ri = 50 and Re = 40. It is noted that for n = 0.8 and n =1, increasing the value of Ha leads to a decrease in Nusselt number of the bodies C1 and C2 whereas, for n = 1.4, increasing the value of Ha does not greatly affect the Nusselt number of the two bodies (C1 and C2). From here, we conclude that the shear-thickening fluids have a resistance to the influence of the magnetic field. The obtained results are similar with those seen previously in Laidoudi et al. (2022), Hatič et al. (2021) and Kefayati (2015).

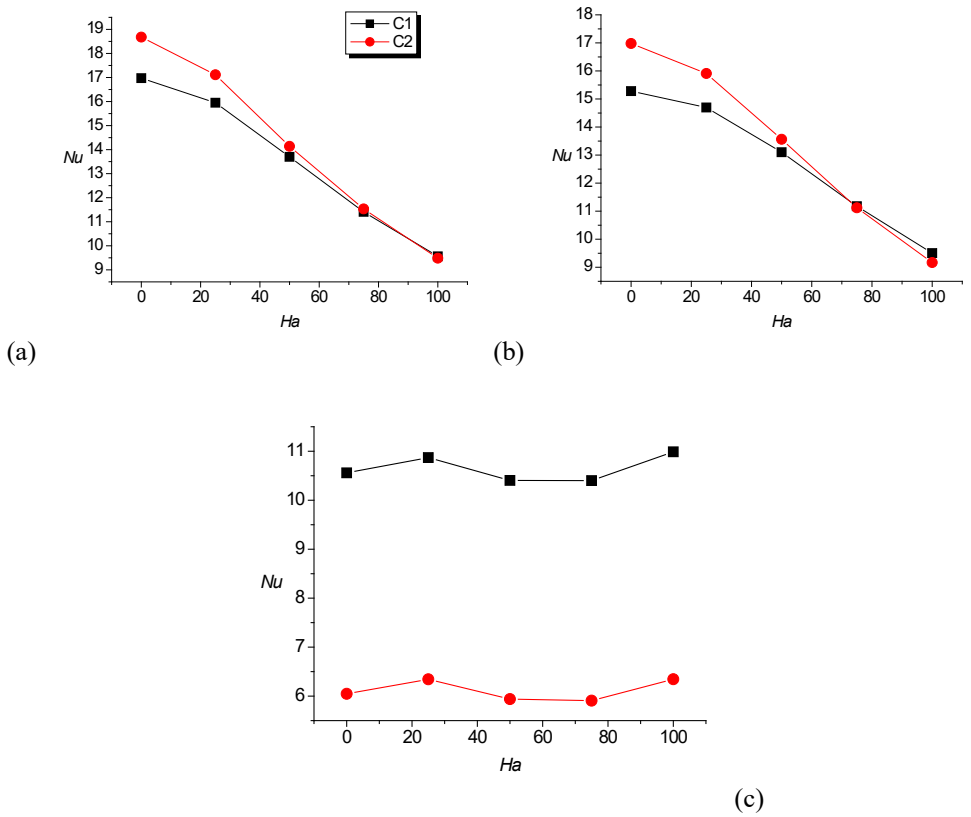

Fig. 11. Variation of Nusselt number of C1 and C2 bodies in terms of Ha for Re = 40 and Ri = 50. (a) for n = 0.8. (b) for n = 1. (c) for n = 1.4.

5. Conclusion

This research aims to present a numerical study of a complex fluid inside a chamber containing two semi-circular bodies and subjected to an external magnetic field. The room has two walls moving horizontally at a constant speed. The study aims to show the movement of the fluid inside the chamber and to determine the heat transfer between the fluid and the hot bodies. The factors studied here are: Re = 1 to 40, Ri = 0 to 100, Ha = 0 to 100 and n = 0.6 to 1.4. Interpretation of the fluid dynamic pattern and its effect on thermal activity was performed by analyzing velocity and temperature contours. The quantitative values of the thermal activity were expressed in terms of the Nusselt number. The determination of the results of this research enables us to note the following points:

- Increasing the value of the Reynolds number and/or Richardson number increases the velocity of the flow in the chamber and strengthens the thermal transfer of the two bodies.
- The heat transfer varies from one body to another and it depends on the values used in initial conditions.
- Increasing the value of power-law index makes the flow more coherent, which reduces the velocity of the flow and delays its thermal activity.

- An increase in the value of the Hartmann number obstructs the movement of the flow, which makes the thermal activity slower.
- The influence of the magnetic field becomes less effective as the power-law index (n) increases.
- Shear-thickening fluids can be used as a medium to suppress the effect of magnetic field on thermal activity.

References

Aboueian-Jahromi J, Nezhad A H, Behzadmehr A, (2011). Effects of inclination angle on the steady flow and heat transfer of power-law fluids around a heated inclined square cylinder in a plane channel. Journal of Non-Newtonian Fluid Mechanics, 166, 1406-1414.

Aissa A, Qasem N A A, Mourad A, Laidoudi H, Younis O, Guedri K, Alazzam A, (2023). A review of the enhancement of solar thermal collectors using nanofluids and turbulators. Applied Thermal Engineering, 220, 119663.

Albensoeder S, Kuhlmann HC, (2005). Accurate three-dimensional lid-driven cavity flow, Journal of Computational Physics, 206, 536-558.

Aliouane I, Kaid N, Ameur H, Laidoudi H, (2021). Investigation of the flow and thermal fields in square enclosures: Rayleigh-Bénard's instabilities of nanofluids. Thermal Science and Engineering Progress, 25, 100959.

Alsabery A I, Sheremet M A, Sheikholeslami M, Chamkha A J, Hashim I, (2020). Magnetohydrodynamics energy transport inside a double lid-driven wavy-walled chamber: Impacts of inner solid cylinder and two-phase nanoliquid approach. International Journal of Mechanical Sciences, 184, 105846.

Anouar Y, Mokhefi A, (2022). Numerical investigation of the nanofluid natural convection flow in a cpu heat sink using buongiorno tow-phase model. Journal of the Serbian Society for Computational Mechanics, 16, 13-42.

Chatterjee D, (2013). MHD mixed convection in a lid-driven cavity including a heated source. Numerical Heat Transfer, Part A: Applications, 64, 235-254.

Chowdhury M, Kumar B V R, (2023). Study of unsteady non-Newtonian fluid flow behavior in a two-sided lid-driven cavity at different aspect ratios. Journal of Non-Newtonian Fluid Mechanics, 312, 104975.

Chowdhury S, Roy P P, Raj M H, Saha S, (2023). Pure mixed convection in a Non-Newtonian fluid filled lid-driven chamber with discrete bottom heating. Case Studies in Thermal Engineering, 49, 103183.

Esfe M H, Saedodin S, Malekshah E H, Babaie A, Rostamian H, (2019). Mixed convection inside lid-driven cavities filled with nanofluids. Journal of Thermal Analysis and Calorimitry, 135, 813–859.

Gangawane K M, Oztop H F, Abu-Hamdeh N, (2018). Mixed convection characteristic in a lid-driven cavity containing heated triangular block: Effect of location and size of block. International Journal of Heat and Mass Transfer, 124, 860–875.

Hansda S, Pandit SK, (2023). Performance of thermosolutal discharge for double diffusive mixed convection of hybrid nanofluid in a lid driven concave–convex chamber. Journal of Thermal Analysis and Calorimetry, 148, 1109–1131.

Hatič V, Mavrič B, Šarler B, (2021). Meshless simulation of a lid-driven cavity problem with a non-Newtonian fluid. Engineering Analysis with Boundary Elements, 131, 86-99.

Herouz K, Laidoudi H, Aissa A, Mourad A, Guedri K, Oreijah M, Younis O, (2022). Analysis of nano-encapsulated phase change material confined in a double lid-driven hexagonal porous chamber with an obstacle under magnetic field. Journal of Energy Storage, 61, 106736.

Hussain S, Mehmood K, Sagheer M, (2016). MHD mixed convection and entropy generation of water–alumina nanofluid flow in a double lid driven cavity with discrete heating. Journal of Magnetism and Magnetic Materials, 419, 140-155.

Hussain S, Öztop H F, (2021). Impact of inclined magnetic field and power law fluid on double diffusive mixed convection in lid-driven curvilinear cavity. International Communications in Heat and Mass Transfer, 127, 105549.

Islam AW, Sharif M A R, Carlson E S, (2012). Mixed convection in a lid driven square cavity with an isothermally heated square blockage inside. International Journal of Heat and Mass Transfer, 55, 5244-5255.

Iftikhar B, Javed T, Siddiqu M A, (2023). Entropy generation analysis during MHD mixed convection flow of non-Newtonian fluid saturated inside the square cavity. Journal of Computational Science, 66, 101907.

Javed T, Iftikhar B, Siddiqui MA, (2023). MHD mixed convection non-isothermal flow and heat transfer analysis of non-Newtonian fluid saturated in I-shaped cavity. Numerical Heat Transfer, Part B, 83, 395-409.

Kareem A K, Gao S, (2017). Mixed convection heat transfer of turbulent flow in a three-dimensional lid-driven cavity with a rotating cylinder. International Journal of Heat and Mass Transfer, 112, 185-200.

Kardgar A, (2021). Numerical investigation of MHD oscillating power-law non-Newtonian nanofluid flow in an enclosure, Eur. Phys. J. Plus, 136, 58.

Kefayati G H R, (2015). FDLBM simulation of mixed convection in a lid-driven cavity filled with non-Newtonian nanofluid in the presence of magnetic field. International Journal of Thermal Sciences, 95, 29-46.

Kefayati G H R, (2016). Simulation of double diffusive MHD (magnetohydrodynamic) natural convection and entropy generation in an open cavity filled with power-law fluids in the presence of Soret and Dufour effects (Part I: Study of fluid flow, heat and mass transfer). Energy, 107, 889-916.

Khanafer K, Aithal SM, (2013). Laminar mixed convection flow and heat transfer characteristics in a lid driven cavity with a circular cylinder. International Journal of Heat and Mass Transfer, 66, 200-209.

Khanafer K, Aithal S M, (2017). Mixed convection heat transfer in a lid-driven cavity with a rotating circular cylinder, International Communications in Heat and Mass Transfer, 86, 131-142.

Laidoudi H, (2020). Buoyancy-driven flow in annular space from two circular cylinders in tandem arrangement. Metallurgical and Materials Engineering, 26, 87-102.

Laidoudi H, Aissa A, Saeed AM, Guedri K, Weera W, Younis O, Mourad A, Marzouki R, (2022). Irreversibility interpretation and MHD mixed convection of hybrid nanofluids in a 3D heated lid-driven chamber. Nanomaterials, 12, 1747.

Laidoudi H, Ameur H, Sahebi S A R, Hoseinzadeh S, (2022a). Thermal analysis of steady simulation of free convection from concentric elliptical annuli of a horizontal arrangement. Arabian Journal for Science and Engineering, 47, 15647–15660.

Laidoudi H, Ameur H, (2020). Investigation of the mixed convection of power-law fluids between two horizontal concentric cylinders: Effect of various operating conditions, Thermal Science and Engineering Progress, 20, 100731.

Laidoudi H, Bouzit M, (2017). The effect of asymmetrically confined circular cylinder and opposing buoyancy on fluid flow and heat transfer. Defect and Diffusion Forum, 374, 18-28.

Laidoudi H, Bouzit M, (2018). The effects of aiding and opposing thermal buoyancy on downward flow around a confined circular cylinder, Periodica Polytechnica Mechanical Engineering, 62, 42-50.

Maneengam A, Laidoudi H, Abderrahmane A, Rasool G, Guedri K, Weera W, Younis O, Bouallegue B, (2022). Entropy generation in 2D lid-driven porous container with the

presence of obstacles of different shapes and under the influences of Buoyancy and Lorentz Forces. Nanomaterials, 12, 2206, 2022.

Mohebbi R, Rashidi MM, (2017). Numerical simulation of natural convection heat transfer of a nanofluid in an L-shaped enclosure with a heating obstacle. Journal of the Taiwan Institute of Chemical Engineers, 72, 70-84.

Nasrin R, Alim MA, Chamkha J A, (2014). Modeling of mixed convective heat transfer utilizing nanofluid in a double lid-driven chamber with internal heat generation. International Journal of Numerical Methods for Heat & Fluid Flow, 24, 36-57.

Nemati H, Farhadi M, Sedighi K, Fattahi E, Darzi A A R, (2010). Lattice Boltzmann simulation of nanofluid in lid-driven cavity. International Communications in Heat and Mass Transfer, 37, 1528-1534.

Oztop H F, Al-Salem K, Pop I. (2011). MHD mixed convection in a lid-driven cavity with corner heater. International Journal of Heat and Mass Transfer, 54, 3494-3504.

Peng Y F, Shiau YH, Hwang R R, (2003). Transition in a 2-D lid-driven cavity flow. Computers & Fluids, 32, 337-352.

Rais A I, Mahmud M J, Hossain M R, Saha S, (2023). Influence of heat generation/absorption on mixed convective flow in a lid-driven chamber with isothermal rotating cylinder. Annals of Nuclear Energy, 182, 109596.

Rashidi MM, Sadri M, Sheremet MA, (2021). Numerical simulation of hybrid nanofluid mixed convection in a lid-driven square cavity with magnetic field using high-order compact scheme. Nanomaterials. 11, 2250.

Selimefendigil F, (2022). Mixed convection in a lid-driven cavity filled with single and multiple-walled carbon nanotubes nanofluid having an inner elliptic obstacle. Propulsion and Power Research, 8, 128–137.

Shuvo M S, Hasib M H, Saha S, (2022). Entropy generation and characteristics of mixed convection in lid-driven trapezoidal tilted enclosure filled with nanofluid. Heliyon, 8, e12079.

Sivanandam S, Marimuthu B, (2023). Numerical study on influence of inclination and sinusoidal heating on magneto-convection in an inclined lid-driven cavity. Multidiscipline Modeling in Materials and Structures, 19, 361-374.

Usman M, Khand Z H, Liu M B, (2019). MHD natural convection and thermal control inside a cavity with obstacles under the radiation effects, Physica A: Statistical Mechanics and its Applications, 535, 122443.

Yeasmin S, Islam Z, Azad A K, Morshed Alam E M, Rahman M M, Karim M F, (2022). Thermal performance of a hollow cylinder with low conductive materials in a lid-driven square cavity with partially cooled vertical wall, Thermal Science and Engineering Progress, 35, 101454.